Lattice Constants and Thermal Expansion Coefficient of Air Clathrate Hydrate in Deep Ice Cores from Vostok, Antarctica

Satoshi Takeya* and Hideki Nagaya

Graduate School of Environmental Earth Science, Hokkaido University, N10 W5, Sapporo 060-0510, Japan

Tetuhiro Matsuyama

Department of Applied Physics, Faculty of Engineering, Hokkaido University, N13, W8, Sapporo 060-8628, Japan

Takeo Hondoh

The Institute of Low-Temperature Science, Hokkaido University, N19 W8, Sapporo 060-0819, Japan

Vladimir Ya. Lipenkov

The Arctic and Antarctic Research Institute, 38 Berung Str., St. Petersburg 199397, Russia

Received: September 17, 1999; In Final Form: November 17, 1999

We measured the temperature-dependent lattice constant of air hydrates in deep ice cores from Vostok, Antarctica, using single-crystal X-ray diffraction. Thus the thermal expansion coefficient was determined, the first for a structure II clathrate hydrate containing small guest molecules. Despite their high dissociation pressures, measurements were done at atmospheric pressure because the air hydrates had stabilized during their original residence at high pressure. At 200 K, the lattice constant and thermal expansion coefficient were 17.20 Å and 44 ($\pm$9) $\times$ 10^{-6} K^{-1}, respectively. This thermal expansion coefficient is approximately equal to that from tetrahydrofuran hydrate, another structure II hydrate, but the lattice constant is 0.3% smaller. Crystal structure refinement determined that the total cage occupancy by air molecules was 0.9.

Introduction

Air hydrates are crystals that can form from air bubbles in polar ice sheets. To reconstruct climates more than several thousand years ago, measurements of the individual gases in air hydrates are essential; however, little is known about how hydrate lattice constants depend on the gases.

Gas hydrates are crystals composed of hydrogen-bonded polyhedra of water molecules, each surrounding one or two guest molecules, and form at low temperature and high pressure. Their crystalline structures are the Stackelberg's structure I composed of 12- and 14-hedra (space group, *Pm*3*n*) and the Stackelberg's structure II composed of 12- and 16-hedra (space group, *Fd*3*m*).[1−4] The lattice constants of structure I and structure II hydrate at 273 K are 12.0 and 17.3 Å, respectively.[5] Air hydrate has structure II with a lattice constant of 17.21 Å at 255 K.[6]

The thermal expansion coefficient of ethylene oxide and tetrahydrofuran (THF) hydrates are significantly larger than that of hexagonal ice (I_h); this, according to constant-pressure molecular-dynamics calculations, is due to anharmonicity in the water−guest molecule interactions.[7,8] Furthermore, calculations for Xe hydrate (structure I)[9] showed that a smaller guest has a more anharmonic water−guest potential and therefore causes a larger thermal expansion. In addition, increasing the temperature has the same effect as increasing the guest size: the expansion coefficient relative to I_h decreases. But, because of high dissociation pressures, thermal expansion of clathrate hydrates with small guest molecules had not been measured.

Air hydrate crystals form where the overburden pressure exceeds the dissociation pressure: at depths greater than 500 m in polar ice sheets. Although they gradually dissociate into air bubbles at atmospheric pressure, the transformation is very slow at low temperatures: during six years of storage, for example, only 0.2% dissociated at −50 °C, increasing to 22.9% at −20 °C.[10] This advantage of air hydrates in Vostok ice cores allowed simpler measurement of their lattice constant at several temperatures.

Experimental Section

We used air hydrate crystals in the Vostok 3G and Vostok 4G cores from Vostok station, Antarctica. The 3G core was drilled from 1980 to 1982 and stored at −20 °C while the 4G core was drilled from 1987 to 1992 and stored below −50 °C.

Ice containing one single crystal of hydrate was carefully cut into a cube one millimeter on edge using a microtome in a −20 °C cold room. The cube was then attached to a fine glass capillary and placed in a thin-walled glass tube filled with silicone oil to avoid sublimation of the ice (Figure 1). An automated four-circle diffractometer equipped with an X-ray source [Rigaku RU-H2R with a Mo target (60 kV $\times$ 200 mA)] collected X-ray intensity data. The diffractometer required a specially designed cooling apparatus (Rigaku) to operate in the room-temperature laboratory.

* Corresponding author. Fax:+81-11-706-7351. E-mail: takeya@hhp2.lowtem.hokudai.ac.jp.

10.1021/jp993344o CCC: $19.00
Published on Web 01/05/2000

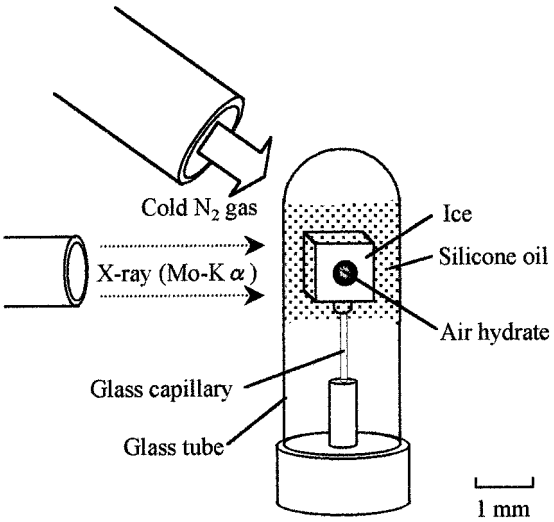

Figure 1. Experimental setup for the X-ray diffraction measurements.

Air hydrate diffraction peaks with 2θ angles between 11.8° and 15.3° were selected because ice crystal peaks should not be in this range. We first estimated the unit cell from these peaks' reciprocal lattice vectors. To determine the lattice constant more precisely, peaks for angles greater than 15.3° for each set of indices (*h, k, l*) were then included. For the refinement of the unit cell, integrated intensities were also measured automatically for indices that had a 2θ angle less than 35°. Structure factor data larger than three times the standard deviation for each structure factor were used, and a spherical absorption correction was made because the hydrate crystal was surrounded by ice.

Following a method used previously,[6] the least-squares refinement of the crystal structure used teXsan software (Rigaku) and started from the positions of the water molecules determined in the previous study of the Dye 3 crystal.[6,11] For guest molecules, off-centered four equivalent sites were assumed for the 16-hedral cage, while a centered single site was used for the 12-hedral cage. These assumptions were introduced by Hondoh et al.[6,11] for the distribution of guest molecules in the cages. For scattering factors of guest molecules, effective scattering factors were calculated for N_2 and O_2 using a free rotor model [12] and averaged to obtain the average guest molecule scattering factor. To determine the site occupancies of the guest molecules, weighted *R* factors, R_W factors, were minimized by varying the site occupancy (0−0.25) for every four sites in the 16-hedral cage and that (0−1.00) for the 12-hedral cage, as well as temperature parameters of both the oxygen atoms in the host lattice and the guest molecules. This minimization used teXsan software after the refinement of the oxygen positions in the host lattice. The site occupancy values for the large (16-hedral) cage in Table 1 are those at the minimum R_W factor and multiplied by 4. To examine the distribution of the guest molecule in the cages, difference synthesis was computed by subtracting out the contribution from water molecules in the host lattice.

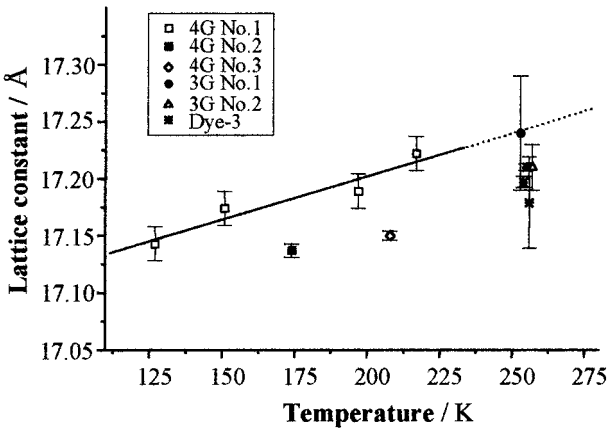

Figure 2. Lattice constants of air hydrates. The solid line is fitted to lattice constant data of specimen 4G No.1. Dye-3 core data are from refs 6 and 12.

Results and Discussion

Lattice constants for six crystals are plotted against temperature in Figure 2. For calculation of the thermal expansion coefficient, linear regression was done using data from specimen 4G No.1 between 127 and 217 K. The error of the individual measurements was ±0.015 Å, or 0.09%. The slope in Figure 2 indicates the lattice constant at 200 K was 17.20 Å, which is 0.05 Å, or 0.3% smaller than that of THF hydrate.[7,8] Moreover, the slope indicates the thermal expansion coefficient was 44 (±9) × 10^{-6} K^{-1}. This is nearly the same as the average thermal expansion coefficient of THF hydrate in this temperature range (49 × 10^{-6} K^{-1}),[7,8] but larger than that of I_h for *a* and *c* axes (31 × 10^{-6} K^{-1}).[13]

For comparison, the lattice constant data from every crystal were extrapolated to 273 K using the thermal expansion coefficient from specimen 4G No.1. The resulting lattice constants range from 17.20 to 17.25 Å (see Table 1): a maximum deviation between specimens of 0.3%.

The pressure in the air hydrates when they were in the ice sheet is the overburden pressure, ranging between 18 and 25 MPa, depending on the depth. However, after recovery of the ice cores, the pressure in the ice must decrease to a lower but unknown pressure. Therefore, the measured constants in Table 1 correspond to those at a pressure between atmospheric and

TABLE 1: Glaciological Data, Lattice Constants, and Crystallographic Values Determined by Structure Refinement of the Hydrate Crystals[a]

	glaciological data			crystallographic data					
							site occupancy		
specimen	core/depth (m)	ice temperature[a] (°C)	age (× k year)	lattice constant[b] at 273 K (Å)	no. of reflections	forbidden reflection	total	(large/small)	R_w
4G No. 1	Vostok4G/2542	−27.4	220	17.26					
4G No. 2	Vostok4G/2542	−27.4	220	17.20	74	(0 0 6)	0.89	(0.82/0.93)	0.080
4G No. 3	Vostok4G/1851	−38.8	130	17.21	60		0.91	(0.94/0.89)	0.050
3G No. 1	Vostok3G/1831	−39.1	130	17.25	43	(0 8 10)	0.8[c]	(0.8/0.8)	0.159
3G No. 2	Vostok3G/1831	−39.1	130	17.23	37	(0 8 10)	0.8[c]	(0.8/0.8)	0.136
Dye-3 (ref 6)	Dye-3/1500	−17.7	5	17.21	52		0.78	(0.75/0.80)	0.057
Dye-3 (ref 11)	Dye-3/1500	−17.7	5	17.22	45		0.77	(0.80/0.75)	0.054
Dye-3 (ref 11)	Dye-3/1500	−17.7	5	17.19	31		0.83	(0.90/0.80)	0.048

[a] Ice temperature is the mean ice temperature at each depth as estimated from data in refs 16 and 17. [b] Lattice constants were extrapolated to 273 K. [c] Assumed constant.

TABLE 2: Observed and Calculated Structure Factors of Specimen 4G No. 2[a]

h	*k*	*l*	2θ	Fo	Fc
0	2	2	6.72	76.22	82.28
1	1	3	7.88	40.83	36.89
0	0	4	9.51	95.45	105.91
2	2	4	11.65	142.20	150.90
1	1	5	12.36	242.92	260.40
3	3	3	12.36	286.09	268.99
0	4	4	13.46	302.60	339.68
1	3	5	14.08	247.32	234.22
2	4	4	14.28	73.68	76.52
0	2	6	15.06	109.81	116.56
3	3	5	15.62	70.21	84.07
2	2	6	15.80	57.04	67.78
1	5	5	17.02	47.23	48.55
1	7	3	18.31	54.33	49.66
3	5	5	18.31	47.23	48.55
0	0	8	19.08	55.81	64.58
3	3	7	19.53	181.03	205.14
4	6	4	19.68	28.80	16.18
0	6	6	20.25	307.11	322.49
2	2	8	20.25	279.85	293.03
1	5	7	20.67	64.87	65.53
0	4	8	21.36	117.44	109.56
1	9	1	21.76	102.72	97.49
3	5	7	21.76	115.96	104.86
2	4	8	21.89	92.32	87.77
4	4	8	23.43	34.52	30.85
1	7	7	23.79	59.52	65.75
3	3	9	23.79	46.95	46.62
1	5	9	24.75	40.11	41.10
3	7	7	24.75	41.57	44.19
2	2	10	24.87	54.46	55.48
6	6	6	24.87	72.59	80.00
3	5	9	25.68	66.05	69.48
2	4	10	26.24	64.00	60.56
0	8	8	27.11	37.61	29.96
1	3	11	27.44	50.39	44.98
1	7	9	27.44	48.77	43.33
2	8	8	27.54	72.95	75.38
4	4	10	27.54	49.35	32.24
0	6	10	27.97	101.29	108.25
6	6	8	27.97	47.21	38.40
3	3	11	28.28	45.03	49.26
3	7	9	28.28	62.07	62.11
6	2	10	28.38	37.40	26.56
0	0	12	28.79	79.82	86.03
4	8	8	28.79	62.62	68.11
1	5	11	29.10	89.41	95.00
7	7	7	29.10	91.72	103.70
2	2	12	29.60	108.71	98.15
4	6	10	29.47	108.58	110.26
3	5	11	29.90	62.85	51.92
5	7	9	29.90	68.75	68.88
0	4	12	30.39	37.72	32.04
2	8	10	31.16	45.23	36.16
1	1	13	31.44	47.88	51.44
5	5	11	31.44	49.36	52.4
1	3	13	32.19	38.33	31.39
3	7	11	32.19	46.39	46.49
4	8	10	32.28	39.1	31.56
3	3	13	32.92	116.85	122.83
8	8	8	33.37	157.05	173.08
1	5	13	33.64	38.48	36.37
5	7	11	33.64	47.16	44.49
4	6	12	33.72	38.5	35.71
0	2	14	34.08	41.96	32.75
0	10	10	34.08	197.33	198.38
6	8	10	34.08	40.91	33.17
1	9	11	34.34	41.36	28.07
3	5	13	34.34	52.31	52.21
2	2	14	34.43	48.01	49.7
0	8	12	34.77	40.49	33.66

[a] Diffraction (006) was excluded because it is forbidden.

25 MPa. Assuming a bulk modulus of 5.6 GPa for the air hydrate,[5] the resulting lattice constant uncertainty is 0.15%.

A related error is from the difference in thermal expansion coefficient between ice and air hydrate. This difference reduces the thermal expansion coefficient from that of an isolated air hydrate crystal because tensile stress is exerted on the hydrate included in ice when the temperature is lowered. By assuming concentric spheres of I_h and air hydrate, this effect was estimated to change the lattice constants in Table 1 by less than 0.1%, i.e., probably less than the linear regression error.

There were no clear correlations between the lattice constants and other crystallographic parameters (see Tables 1 and 2). All air hydrate specimens in this study had Stackelberg's structure II ($Fd\bar{3}m$), but the following forbidden reflections were observed. Crystals in the Vostok 3G cores (kept at −20 °C for about six years) had the forbidden (0 8 10) reflection and R_W factors exceeding 0.10. Crystals from the lower-temperature Vostok 4G cores instead had the forbidden (0 0 6) reflection; however, its R_W factor was less than 0.10. The distributions of the guest molecules in the cages were approximately those found previously:[6,13] a distribution with four maxima in the 16-hedral cages and a centered spherical distribution in the 12-hedral cages.

The different lattice constants might have come from expansion during long-term storage at atmospheric pressure. However, Dye-3 crystals had smaller lattice constants despite being stored in similar conditions (Table 1). Since lattice constants of clathrate hydrates vary with the guest molecules' size, differences in the gas compositions of the air hydrates might affect the lattice constants.[14] However, according to the recent studies on air hydrate formation in ice sheets,[15] the compositions of major gases (N_2, O_2) in the air hydrates at these depths must be close to the present atmospheric value. Thus, we did not find a plausible explanation for the different lattice constants.

Although the accuracy of the present measurements was not sufficient to deduce nonlinearity in the thermal expansion coefficient, the method is useful for structural studies of gas hydrates with a high dissociation pressure. These results could aid measurements in the newly retrieved ice cores from Dome Fuji, Antarctica.

References and Notes

(1) Stackelberg, M. V.; Muller, H. R. *Naturwissenschaften* **1951**, *38*, 456.
(2) Muller, H. R.; Stackelberg, M. V. *Naturwissenschaften* **1952**, *39*, 20.
(3) McMullan, R. K.; Jeffrey, G. A. *J. Chem. Phys*. **1965**, *42*, 2725.
(4) Mak, T. C. W.; Mcmullan, R. K. *J. Chem. Phys*. **1965**, *42*, 2732.
(5) Sloan, E. D., Jr. *Clathrate Hydrate of Natural Gases*, 2nd ed.; Marcel Dekker: New York, 1998.
(6) Hondoh, T.; Anzai, H.; Goto, A.; Mae, S.; Higashi, A.; Langway, C. C., Jr. *J. Inclusion Phenom. Mol. Recognit. Chem*. **1990**, *8*, 17.
(7) Tse, J. S. *J. Phys. (Paris)* **1987**, *48*, C1−543.
(8) Tse, J. S.; McKinnon, W. R.; Marchi, M. *J. Phys. Chem*. **1987**, *91*, 4188.
(9) Tanaka, H.; Tamai, Y.; Koga, K. *J. Phys. Chem. B* **1997**, *101*, 6560.
(10) Uchida, T.; Hondoh, T.; Mae, S.; Shoji, H.; Azuma, N. *Mem. Natl. Inst. Polar Res., Spec. Issue* **1994**, *49*, 306.
(11) Anzai, H. M.S. Thesis, Hokkaido Univ., 1989.
(12) James, R. W. *The Optical Principles of the Diffraction of X-rays*; G. Bell and Sons: London, 1962.
(13) Rottger, K.; Endriss, A.; Ihringer, J.; Doyle, S.; Kuhs, W. F. *Acta Cryst*. **1994**, *B50*, 644.
(14) Davidson, D. W.; Handa, Y. P.; Ratcliffe, C. I.; Ripmeester, J. A.; Tse, J. S.; Dahn, J. R.; Lee, F.; Calvert, L. D. *Mol. Cryst. Liq. Cryst*. **1986**, *141*, 141.
(15) Ikeda, T.; Fukazawa, H.; Mae, S.; Pepin, L.; Duval, P.; Champagnon, B.; Lipenkov, V. Ya.; Hondoh, T. *Geophys. Res. Lett*. **1999**, *26*, 91.
(16) Salamatin, A. N.; Vostretsov, R. N.; Petit, J. R.; Lipenkov, V. Ya.; Barkov, N. I. *Data Glaciol. Stud*. **1998**, *85*, 233.
(17) Gundestrup, N. S.; Hansen, B. L. *J. Glaciol*. **1984**, *30*, 282.